A&A 516, A23 (2010)
DOI: 10.1051/0004-6361/200913449

Astronomy & Astrophysics

Wide-field multi-color photometry of the Galactic globular cluster NGC 1261⋆,⋆⋆

V. Kravtsov[1,2], G. Alcaíno[3], G. Marconi[4], and F. Alvarado[3]

[1] Instituto de Astronomía, Universidad Católica del Norte, Avenida Angamos 0610, Antofagasta, Chile
e-mail: vkravtsov@ucn.cl
[2] Sternberg Astronomical Institute, University Avenue 13, 119899 Moscow, Russia
[3] Isaac Newton Institute of Chile, Ministerio de Educación de Chile, Casilla 8-9, Correo 9, Santiago, Chile
e-mail: inewton@terra.cl; falvarad@eso.org
[4] ESO - European Southern Observatory, Alonso de Cordova 3107, Vitacura, Santiago, Chile
e-mail: gmarconi@eso.org

Received 12 October 2009 / Accepted 4 March 2010

ABSTRACT

Aims. This work studies in more detail the stellar population, including its photometric properties and characteristics, in the rarely studied southern Galactic globular cluster NGC 1261. We focus on the brighter sequences of the cluster's color–magnitude diagram (CMD). Like in our previous works, we rely upon photometry in several passbands to achieve more reliable results and conclusions.
Methods. We carried out and analyzed new multi-color photometry of NGC 1261 in $UBVI$ reaching below the turnoff point in all passbands in a fairly extended cluster field, about $14' \times 14'$.
Results. We found several signs of the inhomogeneity ("multiplicity") in the stellar population. The most prominent of them are: (1) the dependence of the radial distribution of sub-giant branch (SGB) stars in the cluster on their U magnitude, with brighter stars less centrally concentrated at the 99.9% level than their fainter counterparts; (2) the dependence of the location of red giant branch (RGB) stars in the U-$(U-B)$ CMD on their radial distance from the cluster center, with the portion of stars bluer in the $(U-B)$ color increasing towards the cluster outskirts. Additionally, the radial variation of the RGB luminosity function in the bump region is suspected. We assume that both the SGB stars brighter in the U and the RGB stars bluer in the $(U-B)$ color are probably associated with blue horizontal branch stars, because of a similarity in their radial distribution in the cluster. We estimated the metalicity of NGC 1261 from the slope of the RGB in U-based CMDs and the location of the RGB bump on the branch. These metallicity indicators give $[Fe/H]_{ZW} = -1.34 \pm 0.16$ dex and $[Fe/H]_{ZW} = -1.41 \pm 0.10$ dex, respectively. We isolated 18 probable blue straggler candidates. They are more centrally concentrated than the lower red giants of comparable brightness at the 97.9% level. Their photometric characteristics imply that their majority is not consistent with the collisional origin. We also reliably isolated the asymptotic giant branch (AGB) clump and estimated the parameter $\Delta V_{ZAHB}^{clump} = 1.01 \pm 0.06$, that is the difference between the V-levels of the zero age HB and the clump.

Key words. globular clusters: general – globular clusters: individual: NGC 1261

1. Introduction

The southern Galactic globular cluster (GC) NGC 1261 ($\alpha_{2000} = 03^h12^m15\overset{s}{.}3$ and $\delta_{2000} = -55°13'01''$) remains one of the rarely studied GCs up to now, in spite of its moderate central concentration ($c = 1.27$), negligible or no reddening because of the relatively high Galactic latitude ($b = -52\overset{\circ}{.}13$), and the somewhat brighter absolute visual magnitude ($M_V = -7.81$) compared to the most probable value of this characteristic of Galactic GCs (Harris 1996). Although the history of CMD studies of this object spans almost 40 years, it resulted so far in only six publications. The first, scattered photographic CMD reaching the horizontal branch (HB) of the cluster, was obtained by Alcaíno & Contreras (1971) and another one of a higher quality, by Alcaíno (1979). The first CCD photometry of NGC 1261, aimed at estimating the cluster's age, was carried out twenty years ago by Bolte & Marleau (1989). Since then three photometric studies were published in 1990s: Alcaíno et al. (1992) focused mainly on the age determination, based on photometry in three bands; Ferraro et al. (1993) studied the brighter sequences of the CMD, and Zoccali et al. (1998) obtained the luminosity and mass functions of NGC 1261. Yet, Hubble space telescope photometry in the cluster has been carried out by Piotto et al. (2002), among 74 Galactic GCs. Note than our short overview is not concerned with publications dealing with variable stars in NGC 1261 and other particular issues.

In this work, we study for the first time the stellar population of NGC 1261 based on photometry that covers a wide cluster field (approximately $14' \times 14'$) and was conducted in several bands, including measurements in the U bandpass, which is rarely used in investigations of Galactic GCs. In particular, we estimated the cluster metalicity by applying metalicity indicators not previously used in NGC 1261, one of which is related to the U-based CMDs. Also, signs of a probable inhomogeneity of the stellar population in NGC 1261 were found with U photometry in the cluster.

⋆ Based on observations with the 1.3 m Warsaw telescope at Las Campanas Observatory.
⋆⋆ Photometry table is only available in electronic form at the CDS via anonymous ftp to cdsarc.u-strasbg.fr (130.79.128.5) or via
http://cdsweb.u-strasbg.fr/cgi-bin/qcat?J/A+A/516/A23

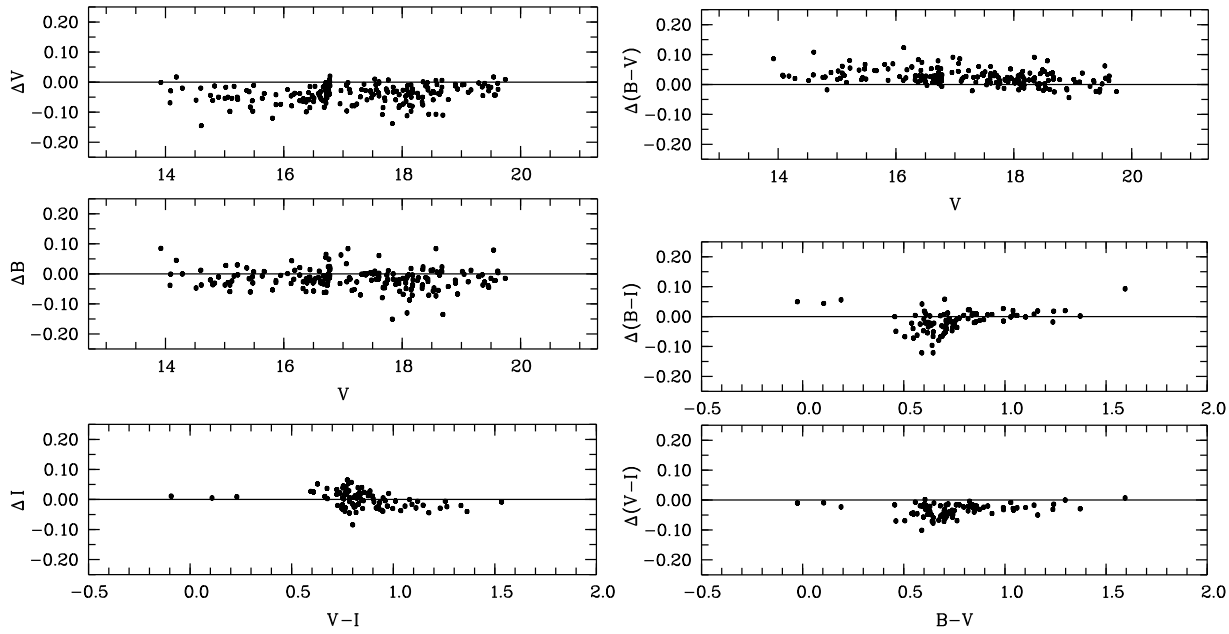

Fig. 1. Comparison of our present photometry of NGC 1261 and the photometry by Stetson (2000) of standard stars in the cluster, taken from the Stetson Photometric Standard Fields; the differences in magnitudes and colors are derived by our data minus those of Stetson.

2. Observations and data reduction

The observations were made on five nights, 1997 December 27/28, 29/30, 30/31, and 1988 January 01/02, 02/03, with the 1.3 m Warsaw telescope, Las Campanas Observatory, using a set of *UBVI* filters and a 2048 × 2048 CCD camera with a gain =3.8 and a readout noise of 5.5e$^-$ rms. The array scale was 0.″417 pixel^{-1}, giving a field of view of 14′ × 14′. The center of the measured field of NGC 1261 was approximately 10″ to the west and 50″ to the south of the cluster center. Flat-field, bias, and dark frames were taken twice per night, at the beginning and at the end. We took a total of 15 frames in *U* (exposure time from 180 s to 720 s), 15 frames in *B* (60 s to 360 s), 15 frames in *V* (40 s to 240 s), and 15 frames in *I* (30 s to 180 s). The observations were gathered with the air mass varying between 1.146 and 1.698. The average seeing on each night, estimated from the observations, was in the range of approximately 1.″1 to 1.″2.

The reductions of CCD photometry were performed at the Isaac Newton Institute and at the European Southern Observatory, ESO, Santiago, Chile. The stellar photometry was carried out separately for all frames with the DAOPHOT/ALLSTAR (Stetson 1987, 1991) and IRAF package[1]. The program stars were detected and measured by applying the usual procedures. To obtain the PSF 20 to 30 stars in each frame, bright but far from saturation, were selected among those without neighbors or defects within the PSF radius. We found that among standard PSFs provided by DAOPHOT, the PENNY2 function enabled us to handle the aberrations specific to individual frames most effectively. The instrumental magnitudes and colors (v, $u-b$, $b-v$, $v-i$) obtained for the measured stars were then transformed to the standard system (V, $U-B$, $B-V$, $V-I$) using 25 standard stars, of which 13 stars (*UBVI*) were from Alcaíno & Liller (1984), seven stars (*UBVI*) from Alcaíno & Liller (1988), and another five stars (*UBV*) from Alcaíno & Contreras (1971).

We used the "least squares" method to calculate a straight line that best fitted the data for these standards stars. The equations used in this study to bring instrumental magnitudes and colors to the standard *UBVI* photometric system are

$$\begin{aligned} V &= v - 0.01(\pm0.01)(b-v) + 0.01(\pm0.03), n = 25, \\ V &= v - 0.03(\pm0.02)(v-i) + 0.05(\pm0.02), n = 15, \\ U-B &= 1.22(\pm0.02)(u-b) - 0.06(\pm0.01), n = 11, \\ B-V &= 1.00(\pm0.02)(b-v) + 0.05(\pm0.01), n = 25, \\ V-I &= 0.92(\pm0.03)(v-i) + 0.11(\pm0.02), n = 15. \end{aligned}$$

The standard errors of the slope coefficients and constants are given along with the number n of standard stars used for the respective transformations.

In our preliminary list we retained only those stars that had at least two measurements per night in each photometric band. We included in our final list only those stars for which at least one color-index was determined. A total of 5481 stars were measured mainly in V. Of these, 2157 stars have $U-B$ color, 5005 have $B-V$, and 4841 have $V-I$[2]. For stars of the brighter sequences, i.e. with $V < 19.0$, the r.m.s. errors are on average ±0.013 in U, ±0.015 in B, ±0.011 in V, and ±0.008 in I.

We compared our photometry with the photometry of Stetson (2000) of around 400 cluster stars in *BVI*, with $V < 20.0$ mag. It was taken from the Stetson Photometric Standard Fields available at http://www3.cadc-ccda.hia-iha.nrc-cnrc.gc.ca/community/STETSON/stds/. We were able to identify 196 stars in the field that were the same. This comparison is shown in Fig. 1. It demonstrates the very good agreement between the two photometries both in magnitudes and colors, over the entire range. Apart from very small or negligible differences in zero-points (within a few hundreds of magnitude) of the photometries, we did not find any notable systematic effect. The comparison also confirms the really good accuracy of our photometry at least up to the limiting V-magnitude (close to the cluster turnoff point)

[1] IRAF is distributed by the National Optical Astronomy Observatory, which is operated by the the Association of Universities for Research in Astronomy, Inc, under cooperative agreement with the National Science Foundation.

[2] The results of our photometry are available in electronic form.

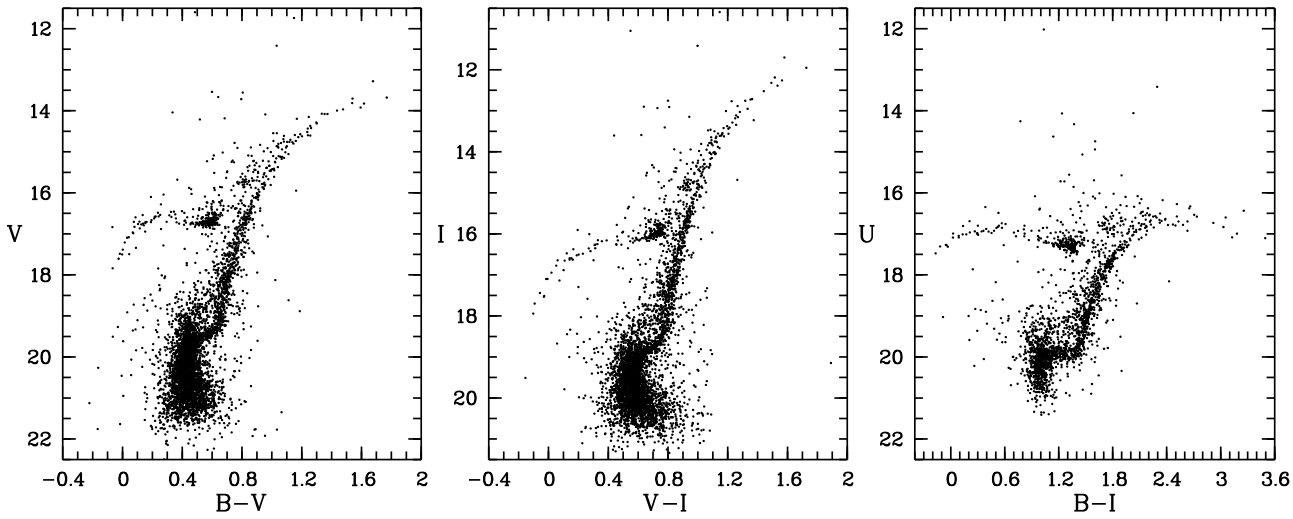

Fig. 2. The V-$(B-V)$, I-$(V-I)$ and U-$(B-I)$ CMDs of the globular cluster NGC 1261 based on $UBVI$photometry of 5481 stars in a $14' \times 14'$ field approximately centered on the cluster.

of the Stetson standard stars. The mean differences between the two photometries in the sense of this work minus that of Stetson (2000), and the number of stars with $V < 20.0$ utilized for the calculations are as follows: $\delta V = -0.04(\pm 0.03)$, 196; $\delta B = -0.02(\pm 0.03)$, 196; $\delta(B-V) = 0.03(\pm 0.03)$, 196; $\delta(V-I) = -0.04(\pm 0.02)$, 88; $\delta(B-I) = -0.01(\pm 0.04)$, 88. The quoted uncertainties are standard deviations.

We also compared our photometry with that by Ferraro et al. (1993) and found 2494 stars in common. Again we did not find any obvious systematic effect in color or in magnitudes, especially for a sub-sample of the brighter stars of this sample with $V < 19.0$. There are only small zero-point offsets: a positive one, within 0.05 mag in the V magnitude, and a negative in the $(B-V)$ color, within a few hundreds of magnitude for this work minus that of Ferraro et al.

3. The color–magnitude diagrams

3.1. General comments

In the panels of Fig. 2 we show the V-$(B-V)$, I-$(V-I)$, and U-$(B-I)$ color-magnitude diagrams (CMDs) constructed with different colors and magnitudes of our photometry of all 5481 stars measured in the observed field of NGC 1261. Due to crowding effects in its inner part, the overall appearance of the CMDs is somewhat worsened by the more scattered sequences in the crowded regions. Increasing the number of blended stars towards the crowded central regions is thought to be (mainly?) responsible for the appearance of numerous stars above the sub-giant branch (SGB) and blueward of the red giant branch RGB, in the form of an apparent sequence. The same feature is also seen in the CMD obtained by Ferraro et al. (1993). In the subsequent analysis of our photometry, we excluded the most crowded central region of NGC 1261.

Because of the fairly high Galactic latitude of the cluster, the contamination of its CMDs by field stars is low. The field stars become detectable only in CMDs of large outer parts of the observed cluster field. In our subsequent analysis we reduced the effect of the contamination on the reliability of the obtained results where it was necessary with multi-color photometry.

3.2. The sub-giant branch

Both a visual inspection of the cluster CMDs and a more objective analysis of our photometry showed not only the apparently thicker SGB in the U-based CMDs than in CMDs with longer wavelength magnitudes with respect to the U, but also the radial variation in the cluster from the mean level of the SGB.

To derive quantitative estimates and thereby to achieve more objective conclusions, we proceeded in the following way. We first obtained a sample of SGB stars. For this purpose the U-based cluster CMD with the $(B-I)$ color-index was used, because it provides the largest separation in a color between the turnoff point (TO) and the lower RGB compared with other available color-indices. To avoid the negative impacts of crowding effect on the obtained results as much as possible, the central part of the cluster, confined within $r = 1\farcm36$ (200 pixels), was excluded from the analysis. Due to fainter magnitudes of SGB stars, the limiting radius of the excluded region is larger than that applied for selection of brighter stars belonging in particular to the HB or RGB bump analyzed below. The SGB of NGC 1261 in the U-$(B-I)$ CMD is virtually horizontal, which facilitates the selection of stars and the subsequent analysis. A raw sample of candidate SBG stars was selected in the color range $\Delta(B-I) = 0.3$ $(1.1 < B-I < 1.4)$ and the magnitude range $\Delta U = 0.4$ mag $(19.7 < U < 20.1)$. To clean it of possible contamination by some field stars and by stars deviating from the TO region and the transitional region between the SGB and lower RGB, the selected stars were plotted in CMDs with magnitudes other than U. The most deviating stars were rejected. The final cleaned sample contained 122 items. We found that the distribution of the selected stars on the U magnitude is apparently rather bimodal than unimodal, with the minimum around $U = 19.90$, which is just at the middle point of the selection magnitude range (Fig. 3). Based on this distribution, the obtained sample of the SGB stars was divided in three sub-samples: (1) a sub-sample of 36 brightest SGB stars in the magnitude range $\Delta U = 0.15$ $(19.70 < U < 19.85)$; (2) a sub-sample of 49 faintest SGB stars in the magnitude range $\Delta U = 0.15$ $(19.95 < U < 20.10)$; (3) a sub-sample of 37 SGB stars with intermediate brightness in the U, falling around the minimum in the magnitude range $\Delta U = 0.10$ $(19.85 < U < 19.95)$. The selection boxes are drawn by the solid line in the U-$(B-I)$ CMD in the upper panel of Fig. 4, where the corresponding selected stars of the

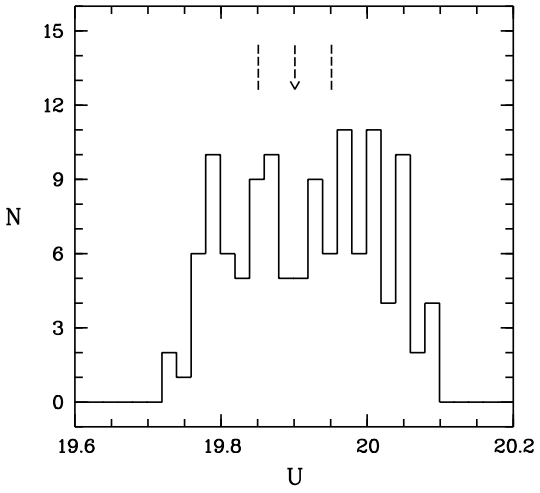

Fig. 3. Distribution of the U magnitude of a total sample of 122 SGB stars isolated in a large field of NGC 1261, excluding its inner part, as described in detail in the text. The arrow shows an apparent minimum at $U = 19.90$ mag, while the two dashed lines are the boundaries of a magnitude range $\Delta U = 0.10$, centered on the minimum, with two neighboring magnitude ranges by $\Delta U = 0.15$ (see explanations in the text).

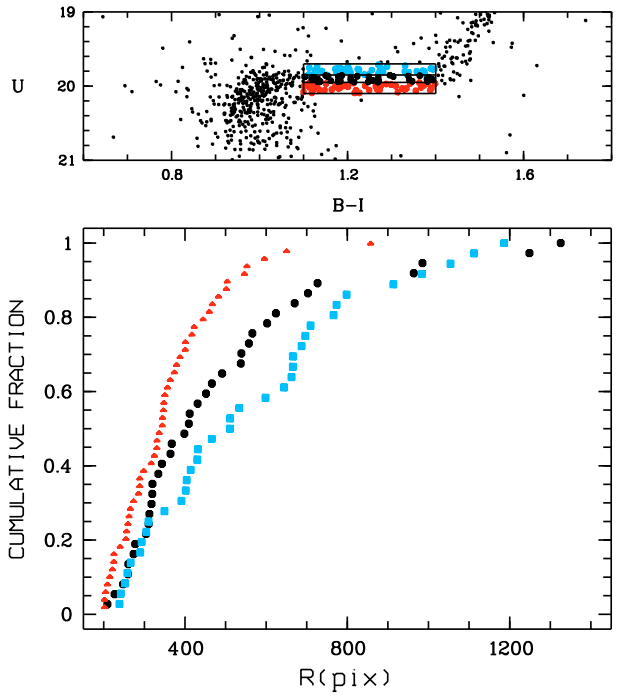

Fig. 4. *Upper panel* shows three sub-samples of the SGB stars isolated in three magnitude ranges in the U-$(B-I)$ CMD of a less crowded field located at radial distances larger than 200 pixels (1.′36) from the cluster center. *Lower panel*: a comparison of the cumulative radial distributions of the three sub-samples of SGB stars; red filled triangles, black filled circles, and blue filled squares denote the sub-samples of the SGB stars with progressively increasing luminosity in the U passband. In both panels, the three sub-samples are shown with the symbols of the same color.

three sub-samples with progressively increasing brightness are denoted by red, black, and blue filled circles, respectively.

The lower panel of Fig. 4 shows the cumulative radial distributions of the three sub-samples of SGB stars. One can see that the faintest sub-giants denoted by (red) filled triangles are more centrally concentrated than their counterparts of intermediate brightness in the U (black filled circles), and obviously yet more centrally concentrated than the brightest SGB stars (blue filled squares). This apparent difference between the distributions is supported by a quantitative estimate based on a Kolmogorov-Smirnov (K-S) test: the difference between the distributions of the brightest and faintest SGB stars is statistically significant at a 99.9% confidence level. Note that the stars falling in the brightest and faintest boxes are (almost) indistinguishable in the V and I magnitudes.

This statistically significant dependence of the radial distribution of SGB stars in NGC 1261 on their U magnitude is strong evidence of the inhomogeneity ("multiplicity") of the cluster stellar population. This inhomogeneity of SGB stars resembles the split of the SGB into two components revealed by Milone et al. (2008) in the globular cluster NGC 1851 and the different radial distribution of stars belonging to the brighter and fainter components of the SGB, found by Zoccali et al. (2009). According to the latter authors, the brighter SGB stars are less centrally concentrated and extend to much larger radial distance in NGC 1851. But the results of Milone et al. (2009) do not support this finding though.

Unfortunately we are not able to draw any definite conclusion about whether or not the revealed differences among the SGB stars are discrete or continuous.

3.3. The red giant branch

The demonstrated evidence of the inhomogeneity of SGB stars is supported by effects found in the RGB.

To analyze the RGB of NGC 1261, we first isolated the most probable RGB stars. We minimized the contamination of the RGB in three steps (1) stars belonging to both the asymptotic giant branch (AGB) and red HB (RHB), (2) a possible few field stars that can appear among the RGB stars in CMD with a given color-index, but are displaced from the sequence on CMDs with other color-indices or/and on the two-color diagrams or (3) stars showing a considerable deviation from the sequence's fiducial line due to photometric error. For this purpose we used the advantage of a multi-color photometry and proceeded like this. In the V-$(B-I)$ CMD we fitted the mean locus of the RGB with a polynomial applying corresponding commands in the MIDAS system. We then linearized the RGB by subtracting for each star the color of the mean locus at its luminosity level from the star's color-index. We left only those stars that satisfied our selection criterion: their deviations $\delta(B-I)$ from the mean locus did not exceed ± 0.06 mag in the total luminosity range of the RGB from its base to the tip. These conditional boundaries of the RGB in the color-index separate the bulk of its stars from the majority of stars belonging to both the AGB and the RHB and are close to the mean errors in the colors along the RGB. It cannot be excluded that some of stars really belonging to the RGB near its tip were rejected or that contrarily some AGB stars merging with those in the upper RGB near its tip were left. The isolated stars were then plotted in CMDs with other color-indices to reject a few of the stars deviating most from the RGB.

Based on the finally obtained sample of 448 RGB stars (which have measurements at least in two passbands, B and V), we were able to develop and reinforce the result on the inhomogeneity of SGB stars. We analyzed specially the expected relationship between the photometric and spatial characteristics of RGB stars. We obtained strong evidence of the inhomogeneity of the population of RGB stars in NGC 1261 as a result. It is based on the dependence of their location in the U-$(U-B)$ CMD on the

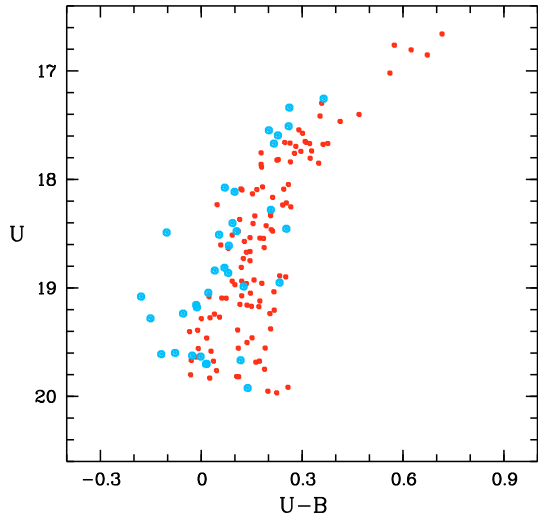

Fig. 5. Comparison of the position in the U-$(U-B)$ CMD of RGB stars from the inner (red dots, $1'.02 < r < 1'.70$) and outermost (blue filled circles, $r > 4'.08$) regions of NGC 1261.

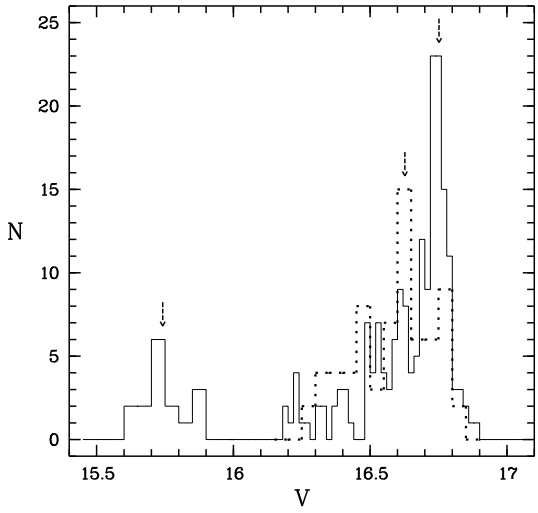

Fig. 6. Distributions of the V magnitude of stars belonging to the RGB bump (dotted line), AGB clump (solid line), and the RHB (solid line at fainter magnitude, with smaller bin size of the histogram); the arrows show the adopted location of the two features and of the ZAHB.

radial distance from the cluster center. Figure 5 demonstrates this dependence from a comparison of the position in this diagram of RGB stars from the inner ($1'.02 < r < 1'.70$; 116 stars) and the outermost (blue filled circles, $r > 4'.08$; 33 stars) regions of NGC 1261. It is evident that red giants at a larger radial distance from the cluster center are on average bluer in the $(U-B)$ color (or/and brighter in the U magnitude). In this connection, we note that Marino et al. (2008) find a dichotomy in Na abundance in a sample of 105 stars in the GC M4 and argue that it must be associated with a CN bimodality. From photometry of the same stars they also showed on the other hand that the CN-weak stars with a simultaneously lower content of Na are systematically bluer, by $\Delta(U-B) = 0.17$ in the U-$(U-B)$ CMD than their CN-strong counterparts with a higher content of Na. This photometric effect resembles that revealed by us in NGC 1261. It is quite difficult to obtain a reliable estimate of the mean separation in the $(U-B)$ color between "bluest" and "reddest" RGB stars. It seems to be of the same order of magnitude as the separation deduced by Marino et al. (2008) for the RGB of M4. However, for NGC 1261 we are inclined to adopt a more conservative estimate of $\Delta(U-B) \sim 0.10$. Hence as a first approximation one can adopt the same reason that led to the segregation of RGB stars in the $(U-B)$ in both GCs, NGC 1261 and M 4. At the same time, we make the opposite suggestion about a probable evolutionary association between the discussed sub-populations of SGB/RGB stars and those belonging to the BHB and RHB. Our suggestion is mainly based on the similarity between the radial distributions in NGC 1261 of the sub-populations of SGB/RGB stars on the one hand and the radial distributions of BHB and RHB stars on the other. More details are given in Sect. 3.4.

With the obtained sample of RGB stars we constructed the RGB luminosity function (LF) in the V magnitude, identified the RGB bump, and isolated a sample of 70 stars that fall in the bump region (BR), i.e. in the magnitude range $\Delta V = 0.6$ $(16.25 < V < 16.85)$, just between the two nearest deepest minima of the LF on both sides of the RGB bump. This fragment of the RGB LF is shown by the dotted line in Fig. 6. The most probable location of the bump was found at $V_{\rm bump} = 16.63 \pm 0.03$. It is close to, but is slightly brighter than $V_{\rm bump} = 16.70 \pm 0.05$ deduced by Ferraro et al. (1993). This difference seems to be primarily due to the larger sample size of the RGB bump stars in our photometry, which therefore allowed us to estimate the location of the RGB bump more confidently by relying on a smaller bin of the LF.

By analyzing the BR LFs in different magnitudes, we found an apparent radial variation in these LFs, which is particularly obvious in the U passband. The BR LFs are shown in Fig. 7, where the solid line is the BR LF of the inner part ($0'.68 < r < 1'.70$; 31 stars) and the dotted line is the BR LF of the outer part of NGC 1261 ($r > 1'.70$, or 250 pixels; 23 stars). To reduce the effect of the increasing photometric error toward the cluster center on the results of our analysis, the innermost region of the cluster containing sixteen stars of the sample was excluded from our consideration. In the panels of Fig. 7, one can fix two kinds of differences between the BR LFs in two parts of the cluster. First, the main maximum that defines the position of the RGB bump dominates in the inner region and almost disappears in the BR LF of the outer cluster part, with the effect apparently more pronounced in the U magnitude. Second, the relative number of stars $N_{\rm brt}/N_{\rm fnt}$ in the brighter and fainter parts of the BR respectively, increases with radial distance from the cluster center. In addition, the BR LFs are systematically more extended toward higher luminosity, by ~0.1 to 0.15 mag, in the outer cluster regions. The adopted boundary between the two parts of the BR in each magnitude ($I_{\rm b}$, $V_{\rm b}$, and $U_{\rm b}$) is marked by the arrow in the three panels of the figure.

To calculate the ratio as carefully as possible, we minimized the effect of the photometric scatter on the estimated ratio as much as possible. For this purpose, we ascribed only those stars to the brighter and fainter parts of the BR whose magnitudes are brighter and fainter respectively, than the adopted boundary magnitudes between the two parts of the BR, i.e. ($I < I_{\rm b}$, $V < V_{\rm b}$, $U < U_{\rm b}$ simultaneously) and ($I > I_{\rm b}$, $V > V_{\rm b}$, $U > U_{\rm b}$ simultaneously). Hence we obtained $N_{\rm brt}/N_{\rm fnt} = 3/23 = 0.13 \pm 0.08$ in the inner region ($0'.68 < r < 1'.70$) in contrast to $N_{\rm brt}/N_{\rm fnt} = 8/12 = 0.67 \pm 0.34$ in the outer part of the cluster ($r > 1'.70$). The radial trend of the ratio is obvious. However, given the errors the difference is marginal. We also estimated the level of statistical significance of the difference between the BR LFs in two parts of the cluster for all three passbands. The K-S test rejects at 85.9%, 85.9%, and 92.4% confidence levels the hypothesis that the BR

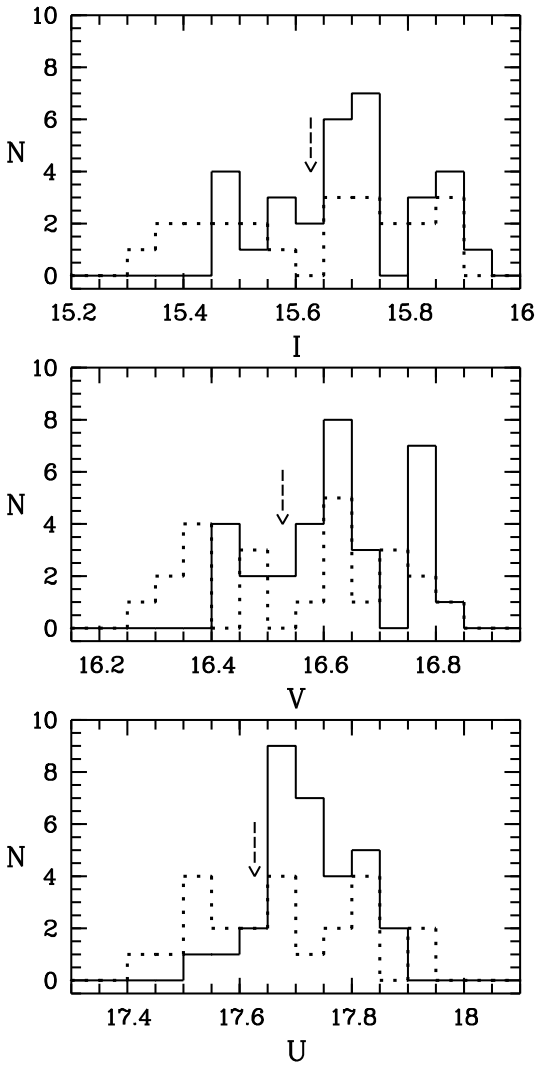

Fig. 7. *Upper, middle*, and *lower panels* show the magnitude distribution of the RGB bump stars in the I, V, and U bands, respectively. In each panel, the solid and dotted lines compare the distributions in the inner ($0\farcm68 < r < 1\farcm70$; 31 stars) and in the outer ($r > 1\farcm70$; 23 stars) regions respectively of the cluster; the arrow indicates the adopted separation between the main and brighter modes of the RGB bump in each plot.

LFs of the inner and outer parts of NGC 1261 are the same distributions in the I, V, and U passbands, respectively. Although the estimated confidence levels are relatively high, especially in the U magnitude, the difference between the BR LFs in the two parts of NGC 1261 are not, strictly speaking, statistically significant, because no confidence levels are greater than 95%. For this reason the discussed apparent radial variations in the BR LFs may be considered as a suspected supplementary sign of the inhomogeneity of RGB stars.

3.4. The horizontal branch

Ferraro et al. (1993) found a probable radial trend of the ratio of the number of BHB stars, $N_{\rm BHB}$, to that of RHB, $N_{\rm RHB}$, in the sense that $N_{\rm BHB}/N_{\rm RHB}$ increases with increasing radial distance from the cluster center. Based on our photometry, which extends to a larger radial distance, we estimate the ratio in two parts of the cluster, located at different mean radial distance: $N_{\rm BHB}/N_{\rm RHB} = 10/77 = 0.13 \pm 0.05$ for $0\farcm68 < r < 1\farcm70$ and $N_{\rm BHB}/N_{\rm RHB} = 13/42 = 0.31 \pm 0.10$ for $r > 1\farcm70$. To avoid an artificial trend, we excluded the most crowded innermost region of the cluster. Although we cannot yet exclude a somewhat higher relative incompleteness of BHB stars in the region located at shorter radial distance, we find the same trend, i.e. RHB stars are presumably more centrally concentrated than BHB ones. Formally, calculated separately in the outermost region, the ratio becomes yet higher, but its statistical significance is negligible due to the very low number of stars used.

We recall that both the SGB stars brighter in the U magnitude and the RGB stars bluer in the $(U - B)$ color are very probably less centrally concentrated in NGC 1261 than their counterparts with distinct photometric characteristics (i.e. the SGB stars fainter in the U and the RGB stars redder in the $(U - B)$, respectively). At the same time, their radial distribution in the cluster resembles just that of BHB stars. Moreover, the relative number of the U-brighter SGB stars and (probably) that of the $(U - B)$-bluer RGB stars is less than 1. This seems to generally agree with the relative number of the BHB stars, i.e. the ratio $N_{\rm BHB}/N_{\rm RHB} < 1$. Given these characteristics, we assume that just the U-bright SGB stars and the $(U - B)$-blue RGB stars are progenitors of of BHB stars in the GC NGC 1261. Note however that Marino et al. (2008) arrived at opposite conclusion about the RGB progeny on the HB: they associated the Na-rich stars, the redder stars in the $(U - B)$ color in the GC M4, with the BHB.

At the end we note that the V-level of the zero age HB (ZAHB) was estimated to be at $V_{\rm ZAHB} = 16.75 \pm 0.05$ (see Fig. 6). Below we use this value to estimate some useful parameters.

3.5. The asymptotic giant branch clump

The CMDs in Fig. 2 show that the number of stars tracing the asymptotic giant branch (AGB) makes it possible to unambiguously identify an important feature, the so-called AGB clump at the base of the branch. It is clearly seen in all diagrams. In the U-$(U - B)$ diagram though it is somewhat stretched along the color axis.

The formation of the AGB clump as well as the well-known RGB bump is caused by a slowing down of the rate of stellar evolution along the given evolutionary sequence(s). For more details concerning the nature of the clump and useful parameters deduced for it from the CMD, as well as for more references related to the subject, we refer in particular to Ferraro et al. (1999) and Sandquist & Bolte (2004). In the present paper, we were able to estimate one of the parameters with good accuracy, namely the difference between the V-levels of the ZAHB and the AGB clump, $\Delta V_{\rm HB}^{\rm clump}$. Because the AGB is poorly populated, the estimates of the given parameter are available for the limited number of GCs.

The AGB clump is located at $V_{\rm clump} = 15.74 \pm 0.03$ (Fig. 6). Taking into account that the ZAHB was estimated to be at $V_{\rm ZAHB} = 16.75 \pm 0.05$, we obtain the parameter $\Delta V_{\rm ZAHB}^{\rm clump} = 1.01 \pm 0.06$.

3.6. Blue stragglers

Relying on four-color photometry of the cluster we were able to isolate blue straggler (BS) candidates more confidently than with two-color photometry. This was achieved with the requirement of simultaneous location of the candidates within the region of the most probable concentration of BSs in several CMDs with different color-indices, namely $(B - V)$, $(V - I)$, and $(B - I)$. Doing so, we isolated 18 probable candidates. This is quite a

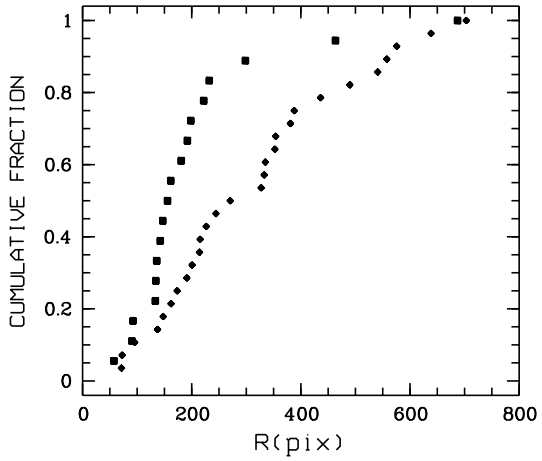

Fig. 8. Comparison of the cumulative radial distributions of blue straggler candidates (filled squares) and lower RGB stars (filled lozenges) falling in narrow magnitude range ($18.8 < V < 19.0$) that is located at the middle level of the magnitude range spanned by the blue straggler candidates ($17.8 < V < 20.0$).

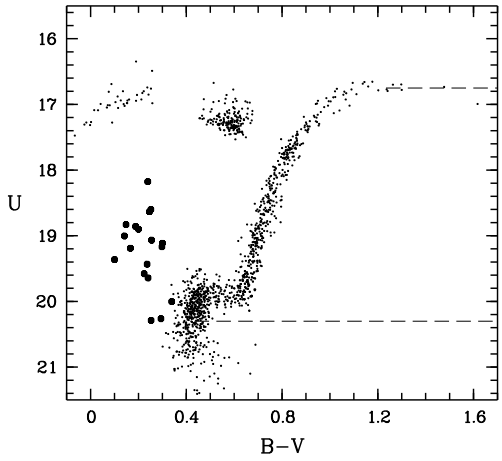

Fig. 9. Composite, cleaned U-$(B-V)$ CMD of NGC 1261 with the most probable blue straggler candidates superimposed (filled squires). the U-levels of the RGB inflection point and the TO point are shown by the upper and lower horizontal dashed lines respectively, aimed at demonstrating the metalicity-sensitive parameter $\Delta U_{\rm TO}^{\rm GB}$.

poor population of BSs. The small number of the found BS candidate can (at least partially) be explained by the increased incompleteness of stars with the same brightness in our photometry, especially in the crowded central part of the cluster. The location of the isolated BS candidates in the U-$(B-V)$ CMD is shown in Fig. 9.

We compared the cumulative radial distribution of the isolated BS candidates with that of a sample of 28 lower RGB stars in a narrow magnitude range ($18.8 < V < 19.0$) that is located at the middle level of the magnitude range spanned by the blue straggler candidates ($17.8 < V < 20.0$). Figure 8 shows the cumulative radial distribution of BS candidates and of the mentioned RGB stars. One can see that the BS candidate are more centrally concentrated than the RGB stars. This apparent obvious difference between both distributions is confirmed by K-S test: the difference is statistically significant at a 97.9% confidence level.

The BS candidates appear in a high range of magnitude (more than 2 mag) in both U and V, but they do not show any notable segregation in the U based two-color diagram, which otherwise might imply distinct groups originating from different BS formation mechanism. We found such two groups in M 80 (Alcaíno et al. 1998) by following the approach of Lauzeral et al. (1993), who in turn had applied the method of Bailyn (1992) to isolate BSs of probable collisional origin. We conclude that among the BS candidates isolated by us in the observed field, excluding the most crowded central region of NGC 1261 where the completeness of faint stars is low and the photometry is shallower, there is none whose origin is consistent with the collisional mechanism.

The isolated BS candidates are marked by flags in the table with the photometric data, which is available in electronic form.

4. Metalicity

To estimate the metalicity of NGC 1261, two methods were applied for the first time for this GC.

We first estimated the metalicity of the cluster by relying on the dependence of the position of the RGB bump on metalicity. This dependence was empirically obtained and demonstrated for the first time by Kravtsov (1989). Here we use the analytically expressed relation between metalicity and $\Delta V_{\rm bump}^{\rm ZAHB}$, the magnitude difference between the bump, and the level of the zero-age HB taken from Ferraro et al. (1999). As we already noted, the most probable locations of the bump and the ZAHB (see Fig. 6) were found to be at $V_{\rm bump} = 16.63 \pm 0.03$ and $V_{\rm ZAHB} = 16.75 \pm 0.05$, respectively. Hence $\Delta V_{\rm bump}^{\rm ZAHB} = -0.12 \pm 0.06$ mag, which is converted to [Fe/H]$= -1.41 \pm 0.10$ dex. Note that the same method applied to the data deduced by Ferraro et al. (1993) gives a somewhat higher metalicity by 0.2 dex. Indeed, they find the RGB bump position at $V_{\rm bump} = 16.70 \pm 0.05$ and the ZAHB level at the same magnitude, $V_{\rm ZAHB} = 16.70 \pm 0.04$. Hence one can calculate $\Delta V_{\rm bump}^{\rm ZAHB} = 0.00 \pm 0.06$ mag, which translates to [Fe/H]$= -1.23$. The same level of the ZAHB and the RGB bump, resulting in this metalicity value is different from our data though: as is seen in Fig. 6, the bump and the expected level of the ZAHB (and even somewhat brighter parts of the HB) are clearly separated, with the bump somewhat brighter.

The above-obtained value of [Fe/H] agrees well with the metalicity deduced from another metalicity indicator, the parameter $\Delta U_{\rm TO}^{\rm RGB}$. In Kravtsov et al. (2007) we defined this parameter as the difference in the U magnitude between the TO and the inflection point of the RGB in the U-$(B-V)$ CMD of GCs in the metal-poor range at $[{\rm Fe/H}]_{\rm ZW} < -1.1$ dex in the scale of Zinn & West (1984). The color difference between the two points is close to $\Delta(B-V) \approx 0.8$ and almost independent of the metalicity in the given metalicity range. We found that the parameter $\Delta U_{\rm TO}^{\rm RGB}$ apparently does not depend on variations in the response curve of the U passband, at least under the conditions of low reddening and the insignificant red leak of the U filters used. However, the parameter very tightly correlates with GC metalicities. We also calibrated $\Delta U_{\rm TO}^{\rm RGB}$ on the metalicity and deduced an analytical relation between $\Delta U_{\rm TO}^{\rm RGB}$ and $[{\rm Fe/H}]_{\rm ZW}$.

We determined the parameter $\Delta U_{\rm TO}^{\rm RGB}$ using the U-$(B-V)$ CMD. However, to estimate the U magnitude of the TO point as carefully as possible, we examined its apparent position in the U-based CMDs with different color-indices and also compared it with the U-level of those stars in the same CMDs, which fall in the TO region in the V-based CMDs where the position of the TO point can be estimated more reliably. We found the U-levels of the RGB inflection point and of the TO

point at $U_{\rm RGB} = 16.75 \pm 0.13$ and $U_{\rm TO} = 20.30 \pm 0.15$, respectively. They are shown by two horizontal dashed lines in the U-$(B-V)$ diagram presented in Fig. 9. Hence the parameter is close to $\Delta U_{\rm TO}^{\rm RGB} = 3.55 \pm 0.20$ mag. Substituting this value in the analytical relation between $\Delta U_{\rm TO}^{\rm RGB}$ and metalicity, we obtained $[{\rm Fe/H}]_{\rm ZW} = -1.34 \pm 0.16$ dex. This value formally coincides with that quoted in the catalog of Harris (1996) and agrees well with the above-obtained quantity. Hence the mean metalicity is $[{\rm Fe/H}]_{\rm ZW} = -1.38 \pm 0.14$ dex.

In the range of previously made estimates of the cluster's metalicity (see, for example, compilations in Alcaíno et al. 1992; and Ferraro et al. 1993) with different methods and indicators, both our estimates (or their mean value) fall near its metal-poor extreme. Therefore our estimates disagree with the values of [Fe/H] ~ -1 dex close to the metal-rich extreme of the cluster metalicity estimates, but agree well with that adopted by Ferraro et al. (1993).

5. Conclusions

We obtained new $UBVI$ photometry of 5481 stars in a wide field, approximately $14' \times 14'$, of the southern, rarely studied GC NGC 1261 below its TO point in all passbands. We exploited this multi-color photometry especially in U passband and its advantages over two-color photometry to further study this GC.

We found two very probable indications and one suspected sign of the inhomogeneity (multiplicity) of the stellar population in NGC 1261. First, there is an obvious dependence of the radial distribution of SGB stars in the cluster on their U magnitude: brighter stars are less centrally concentrated at the 99.9% confidence level and less numerous than their fainter counterparts. Second, RGB stars exhibit a systematically different location in the U-$(U-B)$ diagram at different radial distance from the cluster center: the proportion of stars bluer in the $(U-B)$ (or/and brighter in the U) increases towards the cluster outskirts. Additionally, the distribution of stars on magnitude, particularly in the U band, in the RGB bump region is suspected to change radially in the cluster. We conclude that both the SGB stars brighter in U and the RGB stars bluer in the $(U-B)$ may be associated with the blue BHB, because they are less numerous and less concentrated to the cluster center as compared to their counterparts in the respective evolutionary sequences.

We estimated the metalicity of NGC 1261 by applying metalicity indicators, which were previously not used on this cluster. One of them was recently proposed by us. It is related to deep, U-based CMDs of GCs that simultaneously reach the TO point and trace the upper RGB well with a sufficient amount of stars. The given condition was accomplished by our photometry. We obtained $[{\rm Fe/H}]_{\rm ZW} = -1.34 \pm 0.16$ dex. We also found $[{\rm Fe/H}]_{\rm ZW} = -1.41 \pm 0.10$ by exploiting the dependence of the position of the RGB bump on metalicity. Both estimates agree very well with each other. The resulting mean value of the cluster's metalicity, $[{\rm Fe/H}]_{\rm ZW} = -1.38 \pm 0.14$ dex, is at the metal-poor extreme of the range of previously made estimates on the same metalicity scale obtained by different methods and indicators.

We isolated 18 BS candidates, a quite small population of these stars. They are found to be more centrally concentrated than the lower red giants of a comparable brightness. This difference is statistically significant at the 97.9% confidence level according to the K-S test. Their position in the U-based two-color diagram indicates that the formation of their majority is not due to the collisional mechanism.

Acknowledgements. This research used the facilities of the Canadian Astronomy Data Centre operated by the National Research Council of Canada with the support of the Canadian Space Agency. F.A. is very grateful to Profs. Drs. Felix Mirabel and Massimo Tarenghi, former and actual representatives of ESO in Chile, respectively, for kindly providing living and computing facilities at the ESO office in Santiago, where the observations were reduced. We thank the anonymous referee for useful comments that improved the manuscript.

References

Alcaíno, G. 1979, A&AS, 38, 61
Alcaíno, G., & Contreras, C. 1971, A&A, 11, 14
Alcaíno, G., & Liller, W. 1984, AJ, 89, 1712
Alcaíno, G., & Liller, W. 1988, AJ, 96, 139
Alcaíno, G., Liller, W., Alvarado, F., & Wenderoth, E. 1992, AJ, 104, 1850
Alcaíno, G., Liller, W., Alvarado, F., et al. 1998, AJ, 116, 2415
Bolte, M., & Marleau, F. 1989, A&A, 101, 1088
Bailyn, C. D. 1992, ApJ, 392, 519
Ferraro, F. R., Clementini, G., Fusi Pecci, F., Vitiello, E., & Buonanno, R. 1993, MNRAS, 264, 273
Ferraro, F. R., Messineo, M., Fusi Pecci, F., et al. 1999, AJ, 118, 1738
Harris, W. E. 1996, AJ, 112, 1487
Kravtsov, V. V. 1989, SvA Lett., 15, 356
Kravtsov, V., Alcaíno, G., Marconi, G., & Alvarado, F. 2007, A&A, 469, 529
Lauzeral, C., Auriere, M., & Coupinot, C. 1993, A&A, 274, 214
Marino, A. F., Villanova, S., Piotto, G., et al. 2008, A&A, 490, 625
Milone, A. P., Bedin, L. R., Piotto, G., et al. 2008, ApJ, 673, 241
Milone, A. P., Stetson, P. B., Piotto, G., et al. 2009, A&A, 503, 755
Piotto, G., King, I. R., Djorgovski, S. G., et al. 2002, A&A, 391, 945
Sandquist, E. L., & Bolte M. 2004, ApJ, 611, 323
Stetson, P. B. 1987, PASP, 99, 191
Stetson, P. B. 1991, DAOPHOT II Users Manual
Stetson, P. B. 2000, PASP, 112, 925
Zinn, R., & West M. J. 1984, ApJS, 55, 45
Zoccali, M., Piotto, G., Zaggia, S. R., & Capaccioli, M. 1998, A&A, 331, 541
Zoccali, M., Pancino, E., Catelan, M., et al. 2009, ApJ, 697, L22